

Hyperosmoregulation in the red freshwater crab *Dilocarcinus pagei* (Brachyura, Trichodactylidae): structural and functional asymmetries of the posterior gills

Horst Onken* and John Campbell McNamara

Departamento de Biologia, Faculdade de Filosofia, Ciências e Letras de Ribeirão Preto, Universidade de São Paulo, Avenida Bandeirantes 3900, Ribeirão Preto 14040-901, São Paulo, Brasil

*e-mail: onkenh@ffclrp.usp.br

Accepted 24 October 2001

Summary

The osmotic and ionic status of the haemolymph and the structural and ion-transport characteristics of the posterior gills of *Dilocarcinus pagei*, a hololimnetic crab, were investigated. Haemolymph osmolality was 386 ± 18 mosmol kg⁻¹, while [Na⁺] and [Cl⁻] were 190 ± 13 and 206 ± 12 mmol l⁻¹, respectively; [K⁺], [Ca²⁺] and [Mg²⁺] were 9.7 ± 0.7 , 10.2 ± 0.5 and 2.8 ± 0.4 mmol l⁻¹, respectively (means \pm S.E.M., $N=12-17$). The gill lamellae possess a central, osmiophilic area, which exhibits a marked structural asymmetry. The thick (18–20 μ m) proximal epithelium is characterised by basal invaginations and a few apical vesicles, while the thin (3–10 μ m) distal epithelium consists of apical pillar cell flanges populated by vesicles and membrane invaginations. Isolated gills, bathed and perfused with NaCl saline, spontaneously generate a negative transbranchial potential difference

(V_{te}), which stabilises at positive or negative values. Ouabain shifts V_{te} to more positive values. When mounted in an Ussing chamber, distal split lamellae generate a negative, Cl⁻-dependent short-circuit current (I_{sc}). Na⁺ substitution leads to more negative values of I_{sc} . Internal ouabain is without effect, while diphenylamine-2-carboxylate and acetazolamide abolish I_{sc} . Proximal split lamellae show a positive, Na⁺-dependent I_{sc} , which decreases after internal application of ouabain. These data suggest that the thin epithelium actively absorbs Cl⁻, while the thick epithelium actively absorbs Na⁺.

Key words: Crustacea, red freshwater crab, *Dilocarcinus pagei*, haemolymph, osmolality, ion concentration, gill, transbranchial potential difference, split gill lamellae, Ussing chamber, short-circuit current.

Introduction

Although the true freshwater crabs constitute an abundant and highly successful decapod group, their osmoregulatory capability has been studied mainly from the whole-animal perspective, and little information is available concerning their physiological mechanisms of osmotic and ionic regulation. Like the diadromous crabs that migrate between sea water and fresh water during their life cycle, the hololimnetic Brachyura also maintain large, outwardly directed osmotic and ionic gradients (see Mantel and Farmer, 1983). However, diffusive salt loss and osmotic water entry across the body surfaces of these crabs are reduced by their low permeability to passive salt and water movements (Shaw, 1959; Harris, 1975; Greenaway, 1981; Morris and Van Aardt, 1998).

Unlike the freshwater Macrura, the freshwater crabs do not appear to have evolved the ability to produce dilute urine. Their particularly low rate of iso-osmotic urine production seems not to depend solely on the low water permeability of the body surfaces since reabsorption of iso-osmotic fluid by the antennal gland also reduces urine volume. This strategy, apparently typical of freshwater crabs, may be a water-conserving adaptation to amphibious life (Greenaway, 1981; Harris, 1975; Morris and Van Aardt, 1998). However, since a reduced flow

of iso-osmotic urine also conserves salt, this same adaptation reduces dependence on the mechanisms of active NaCl absorption from the freshwater medium that counterbalance diffusive losses.

Hyperosmoregulating Crustacea compensate for passive salt loss in dilute media by actively absorbing NaCl across their gill epithelia (for reviews, see Péqueux et al., 1988; Péqueux, 1995). In diadromous crabs from marine and brackish waters, these organs, which play vital roles in gas exchange, in osmotic and ionic regulation, in pH regulation and in the excretion of N₂ compounds, have been investigated from the whole gill to the molecular level, employing a wide variety of techniques (for a review, see Taylor and Taylor, 1992). In contrast, investigations of the gills of the hololimnetic or true freshwater crabs have been limited, and gill ultrastructure has been examined only in *Potamon niloticus* (Maina, 1990). No structural differences regarding the gills of other hyperosmoregulating crabs are evident. Freshwater crabs absorb salt against considerable ionic gradients: the external sodium concentration at which half-maximal uptake occurs is less than 0.2 mmol l⁻¹, which is clearly lower than for brackish-water animals. Consistent with the reduced passive salt loss

typical of freshwater crabs, the maximal rate of sodium uptake in whole crabs ($<2 \mu\text{mol g}^{-1} \text{h}^{-1}$) is also lower than that for brackish-water animals (see Morris and Van Aardt, 1998; Potts and Parry, 1964).

Dilocarcinus pagei Stimpson is a hololimnetic, trichodactylid crab endemic to the Amazon and Paraguai/Paraná river basins of South America (Magalhães, 1991). Virtually nothing is known of its osmotic and ion-regulatory capabilities. In the present investigation, we evaluated the haemolymph osmotic and ionic status and analysed the microanatomy and ion-transport characteristics of the posterior gills in this species. Our findings reveal novel structural and physiological asymmetries that underlie the ion-transport capabilities of these gills, disclosing adaptations that may have contributed to the successful invasion of the freshwater biotope by the trichodactylid crabs.

Materials and methods

Crabs

Intermoult *Dilocarcinus pagei* Stimpson, measuring 4.5–5.5 cm in carapace width, were collected from a freshwater reservoir in São José do Rio Preto (São Paulo State, Brazil). In the laboratory, the animals were kept at 20–25 °C on a natural light:dark photoperiod in large tanks containing aerated tap water to a depth of approximately 10 cm; this was replaced 2–3 times a week. Aquatic plants and hollow bricks provided refuge and free access to a dry surface, respectively. The crabs were fed lettuce and/or beef three times a week.

Before killing the crabs, a haemolymph sample of approximately 3 ml was collected *via* the arthroal membrane of the posterior-most pereopod using an insulin syringe coupled to a 28-6 gauge needle. The samples were stored in individual vials at –25 °C until ion concentration analysis.

To obtain the gills, the crabs were quickly killed by destroying the dorsal brain and the ventral ganglion with a large pair of scissors. The carapace was removed, and the gills were excised at their bases with a pair of fine scissors and removed with tweezers. The gills were used immediately for the structural analysis and physiological experiments.

Haemolymph osmolality and ionic composition

Haemolymph osmolality was measured in 10 μl samples using a Wescor 5500 vapour pressure micro-osmometer. Na^+ , K^+ , Ca^{2+} and Mg^{2+} concentrations were measured by atomic absorption spectroscopy (GBC 933AA spectrophotometer) in 10–20 μl samples diluted 1:150–1:5000 times in distilled water. Cl^- concentration was measured in 10 μl haemolymph samples by microtitration against mercuric nitrate using *s*-diphenylcarbazone as the indicator (Santos and McNamara, 1996).

Microscopic studies

After dissection on ice, the gills were immediately perfused *via* the afferent vessel over a 2–3 min period with 1 ml of ice-cold primary fixative containing (in mmol l^{-1}):

paraformaldehyde, 200; glutaraldehyde, 250; Na^+ , 100; K^+ , 10; Ca^{2+} , 13; Mg^{2+} , 2 (as chlorides); buffered in 100 mmol l^{-1} sodium cacodylate at pH 7.5. Medial portions of selected gills consisting of approximately five lamellae each were then fixed on ice in fresh primary fixative for 1.5 h. After rinsing in buffered saline alone (3 \times 5 min), the gill lamellae were post-fixed in 1% osmium tetroxide in buffered saline for 1 h, dehydrated in an ethanol/propylene oxide series and embedded in Araldite 502 resin. Thick (0.5 μm) sections were prepared using a Porter-Blum Sorvall MT-2B ultramicrotome and stained with 1% Methylene and Toluidine Blue in 1% aqueous borax.

Measurement of transbranchial voltage

To perfuse an isolated gill, the afferent vessel was connected by a fine polyethylene catheter (0.6–1.2 mm outer diameter) to a perfusion system, and the gills were flushed in a Petri dish under a binocular microscope for 1–2 min with saline containing (in mmol l^{-1}): NaCl , 200; NaHCO_3 , 2; KCl , 5; CaCl_2 , 10; glucose, 5; Hepes, 5; at pH 7.6 (Tris). A second catheter was inserted into the efferent vessel, and both catheters were then fixed in position with a small Lucite clamp covered with smooth neoprene to avoid gill damage and to isolate the gill interior from the bathing medium. The gill was bathed in a beaker containing approximately 50 ml of aerated saline and was perfused by gravity flow, the perfusate being collected in a second beaker. In 22 experiments, the mean rate of perfusion was $21 \pm 4 \text{ ml h}^{-1}$. Perfusion rate was verified every 15 min for constancy.

To measure the transepithelial voltage (V_{te}) generated by the perfused gills, two calomel electrodes were connected *via* agar bridges (3% agar in 3 mol l^{-1} KCl) to the beakers containing the bath and perfusate. V_{te} was measured using a digital multimeter (model 8050A, Fluke, USA), the reference electrode being placed in the perfusate (internal side), and was recorded every minute for periods of up to 8 h.

Measurements with whole gill lamellae, split gill lamellae and isolated cuticles

Gill lamellae were isolated from a medial portion of the whole gills. Split gill lamellae were obtained by mechanically separating the two halves of a single gill lamella using two pairs of ultra-fine tweezers (see Schwarz and Graszynsky, 1989; Onken and Riestenpatt, 1998). To obtain isolated cuticles, the epithelium was carefully removed from a split lamella preparation with a blunt micro-scraper. All manipulations and mounting of the preparations in a modified Ussing chamber were performed under a stereomicroscope.

A surface area of 0.01 cm^2 was exposed to the chamber compartments (approximately 50 μl volume) bathing the external and internal surfaces of the split gill lamella. Both chamber compartments were continuously perfused with aerated saline by gravity flow (approximately 2 ml min^{-1}). When Na^+ -free saline was used, NaCl was substituted by choline chloride and NaHCO_3 by KHCO_3 . In Cl^- -free saline, NaNO_3 , KNO_3 and calcium gluconate served as Cl^- substitutes.

Table 1. Haemolymph osmolality and ion concentrations in the red river crab *Dilocarcinus pagei*, in a variety of freshwater crab species from Africa and the Indo-Pacific and in selected freshwater Crustacea

	Osmolality (mosmol kg ⁻¹)	[Na ⁺] (mmol l ⁻¹)	[Cl ⁻] (mmol l ⁻¹)	[K ⁺] (mmol l ⁻¹)	[Ca ²⁺] (mmol l ⁻¹)	[Mg ²⁺] (mmol l ⁻¹)	Reference
<i>Dilocarcinus pagei</i>	386±18	190±13	206±12	9.7±0.7	10.2±0.5	2.8±0.4	This study
<i>Potamonautes warreni</i>	636	238	272	4.6	13	4.7	Morris and Van Aardt (1998)
<i>Potamon niloticus</i>	525	270	265	6.4	15.7	4.7	Mantel and Farmer (1983)
<i>Potamon edulis</i>	540	250	210				Mantel and Farmer (1983)
<i>Sudanonautes africanus</i>	500	260	240	8.4	12.7		Mantel and Farmer (1983)
<i>Paratelpusa hydrodromus</i>	480	210	240	5.9	11.8	10.6	Mantel and Farmer (1983)
<i>Holthuisana transversa</i>	620	330	255	6.8	7.8	7.8	Mantel and Farmer (1983)
<i>Astacus astacus</i>	426	205	190	4.6	10		Mantel and Farmer (1983)
<i>Orconectes Limosus</i>	425	245	240	5.5	17.5	2.8	Mantel and Farmer (1983)
<i>Macrobrachium olfersii</i>	340	154	170	5.0	5.5	1.0	McNamara et al. (1990); Lima et al. (1997)
<i>Gammarus duebeni</i>	480	250	225	6			Mantel and Farmer (1983)
<i>Triops longicaudatus</i>	135	74	56.2	4,5	1,7	0.9	Mantel and Farmer (1983)

Data for *D. pagei* are means ± S.E.M. (N=12–17).

For voltage measurements, calomel electrodes were connected via agar bridges (3% agar in 3 mol l⁻¹ KCl) to both sides of the preparation, the distance from the bridge tip to the tissue being less than 1 mm. The reference electrode was placed in the internal bath. Silver wires coated with AgCl served as electrodes to apply current for short-circuiting (i.e. measurement of the short-circuit current, I_{sc}) through an automatic clamping device (model VCC 600; Physiologic Instruments, USA). The conductance of the preparations (G_{te}) was calculated from imposed voltage pulses (ΔV) and the resulting current deflections (ΔI). The data were recorded continuously on a chart recorder (type 3229 I/85; Linseis, Germany).

Chemical reagents

All reagents were of analytical grade. Unless mentioned otherwise, all substances were purchased from Labsynth (Diadema, São Paulo, Brazil). Choline chloride, calcium gluconate and acetazolamide were from Sigma, and KNO₃ and diphenylamine-2-carboxylate (free acid) were obtained from Fluka. Ouabain was from Serva, and agar agar, Hepes and Tris were purchased from Roth (Karlsruhe, Germany).

Statistical analyses

All data are given as the mean ± standard error of the mean (N). Differences between mean values were compared using Student's *t*-test ($P=0.05$).

Results

Haemolymph osmolality and ionic concentrations

Haemolymph osmolality was 386±18 mosmol kg⁻¹ (N=13), while Na⁺ and Cl⁻ concentrations were 190±13 (N=12) and 206±12 mmol l⁻¹ (N=17), respectively. Haemolymph K⁺ concentration was 9.7±0.7 mmol l⁻¹ (N=12), and Ca²⁺ and Mg²⁺ concentrations were 10.2±0.5 and 2.8±0.4 mmol l⁻¹ (N=17), respectively (see Table 1).

Gill microanatomy

Dilocarcinus pagei has eight pairs of phyllobranchiate gills (Fig. 1A). The anterior-most gills, gills 1 and 2 (G1 and G2), are minute and disposed orthogonally to the others; G8 is the posterior-most gill. G1–G5 are designated anterior gills, while G6–8 are considered posterior gills (Fig. 1B). The gill formula is: G1 arthrobranch, G2 podobranch, G3 and G4 arthrobranches with a common insertion point, G5 and G6 arthrobranches with a common insertion point, G7 pleurobranch and G8 pleurobranch. The lamellae comprising the anterior gills are pseudo- to asymmetrical (Fig. 1C), while those constituting the posterior gills are bilaterally symmetrical (Fig. 1D). The lamellae lie slightly staggered on either side of an elongate, central gill shaft containing the afferent and efferent vessels located, respectively, at the epibranchial and hypobranchial gill margins (Fig. 1C,D).

In paraformaldehyde/glutaraldehyde/OsO₄-fixed whole lamellae of gills 6–8, a large, very well defined, osmiophilic area is evident (Fig. 1D). This region reflects an underlying, thick epithelium that exhibits structural features typical of a transporting epithelium (see below). The total lamellar area occupied by this dense area within the posterior gills clearly decreases from posterior to anterior: 79.5±1.8% (N=5) in gill 8, 46.0±5.5% (N=6) in gill 7 and 34.0±3.1% (N=5) in gill 6. A distinct, although less-dense, area occupies 73.7±0.7% (N=4) of the lamellae in anterior gill 4 (Fig. 1C).

Posterior gill 7 was examined by light microscopy to provide a detailed analysis of the lamellar microanatomy. Near the central shaft, the lamellae are approximately 30 µm thick and contain a tenuous (4–5 µm thick), continuous, intralamellar septum that separates the two thin epithelia underlying the cuticle on either side of the lamella (Fig. 1E). Distally from the central axis, the septum becomes finer and discontinuous, disappearing approximately 80 µm from the gill shaft. At this point, the lamellae thicken to approximately 45 µm, and the opposing epithelial layers become conspicuously

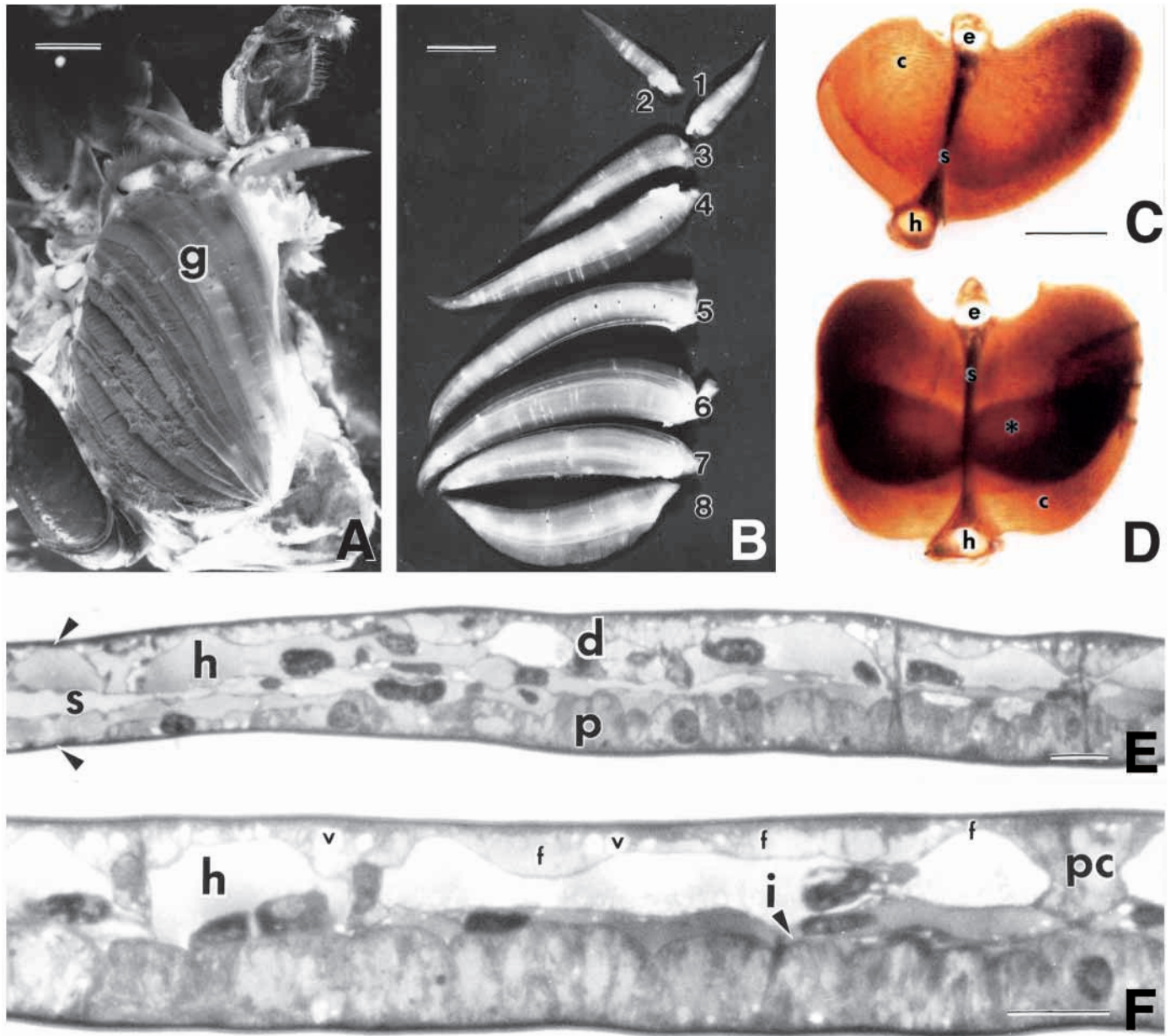


Fig. 1. (A–F) Anatomical and histological features of the gills of the hololimnetic trichodactylid crab *Dilocarcinus pagei*. (A) Macroscopic view of the eight gills (g) *in situ* in the left branchial chamber after removal of the carapace. Scale bar, 5 mm. (B) Phyllobranchiate gills 1–8 (1–8) arranged according to insertion sequence along the antero-posterior body axis. Scale bar, 5 mm. (C,D) Epoxy-embedded whole mounts of paraformaldehyde/glutaraldehyde/OsO₄-fixed lamellae from anterior gill 4 (C) and posterior gill 7 (D). The dense osmiophilic areas (*) in gill 7 reflect an underlying, thick transporting epithelium (see E,F). A clearly less-dense area is also seen in anterior gill 4. Afferent epibranchial (e) and efferent hypobranchial (h) vessels and haemolymph channels (c) originating on either side of the gill shaft (s) are visible. Scale bar, 1 mm. (E) Micrograph of a 0.5 μ m thick epoxy section taken transversely across a lamella from posterior gill 7. An intralamellar septum (s) in the haemolymph space (h) separates the two thin epithelia (arrowheads) near the gill shaft (left side, not visible). Approximately 80 μ m from the shaft, the epithelial layers become asymmetrical: 3–10 μ m thick on the distal side (d) and 18–20 μ m on the proximal side (p). Scale bar, 20 μ m. (F) Micrograph of a 0.5 μ m thick section taken transversely through the osmiophilic region of a lamella from posterior gill 7. The dense, thick proximal epithelium is characterised by numerous basal invaginations (i) and a few apical vesicles. The thin distal epithelium consists of the extensive apical flanges (f) of the pillar cells (pc), populated by numerous vesicles (v) and apical invaginations. h, haemolymph space. Scale bar, 20 μ m.

asymmetrical: on the proximal side, which faces the gill insertion point, the lamellar epithelium is notably thicker (18–20 μ m) than on the distal side (3–10 μ m), which faces the gill tip (Fig. 1E). The dense proximal epithelium (Fig. 1F) is

characterised by basal invaginations and a few apical vesicles. The thin distal epithelium (Fig. 1F) is characterised by the extensive apical expansions of the frequent pillar cells in the form of thin flanges, populated by vesicles and invaginations

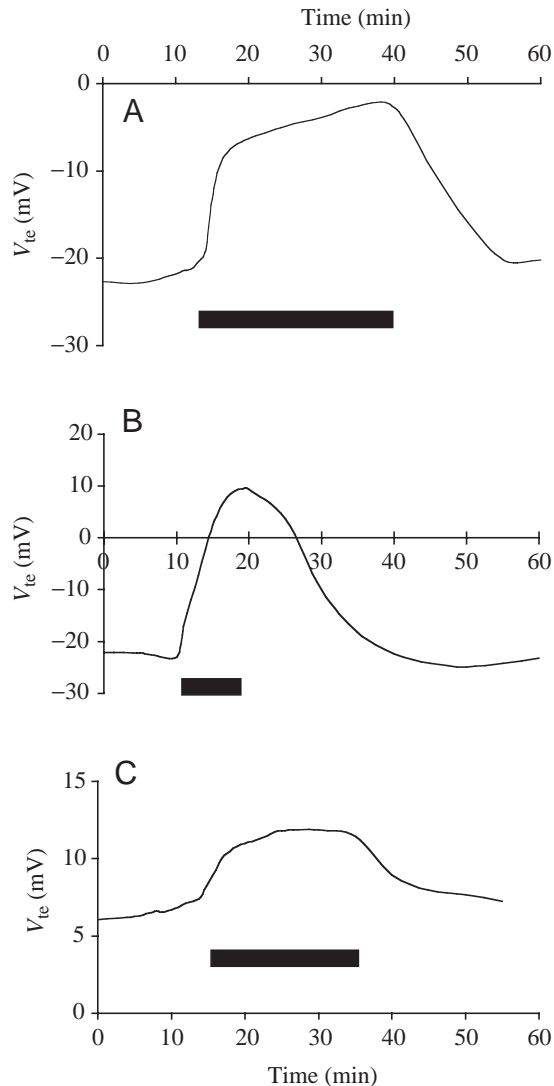


Fig. 2. (A–C) Time courses of the electrical potential difference (V_{te}) across three different, perfused, whole posterior gills, demonstrating examples of the different responses to ouabain (2 mmol l^{-1} , black bars) added to the perfusate. V_{te} was measured as the external potential with respect to the internal medium. An identical NaCl saline was used in the bath and perfusate.

of the apical membrane. The pillar cell bodies extend across the haemolymph space, abutting on the thick proximal epithelium (Fig. 1F).

Electrical potential differences of isolated and perfused posterior gills

Posterior gills, perfused and bathed with NaCl saline, spontaneously generated a negative transepithelial voltage (V_{te}) of $-16 \pm 4\text{ mV}$ ($N=22$), which stabilised after 30 min at $-11 \pm 2\text{ mV}$ in 17 preparations, and at positive values ($+5 \pm 3\text{ mV}$; $N=5$) in five other gills. The addition of ouabain (2 mmol l^{-1}) to the perfusate significantly reduced the transepithelial voltage from -13 ± 3 to $+1 \pm 2\text{ mV}$ ($N=8$; $P < 0.05$). The time courses of the voltage changes in individual gills

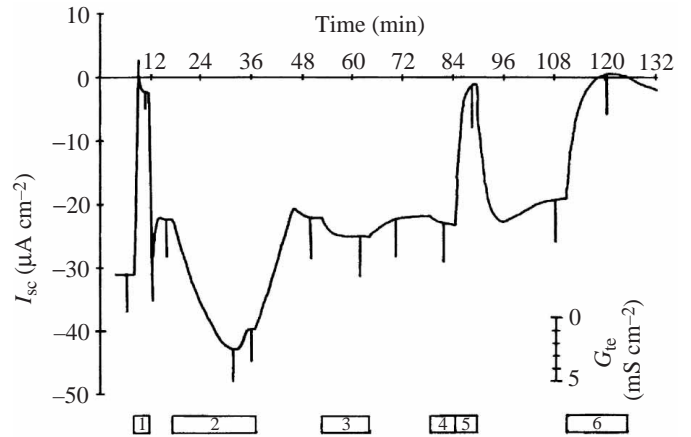


Fig. 3. Representative time course of the short-circuit current (I_{sc}) across a split distal lamella of a posterior gill with NaCl saline on both sides. The following manipulations were performed: 1, substitution of Cl^- on both sides of the preparation; 2, substitution of Na^+ on both sides of the preparation; 3, addition of ouabain (2 mmol l^{-1}) to the internal bathing medium; 4, addition of dimethylsulphoxide (DMSO, 0.2%) to the internal medium; 5, addition of diphenylamine-2-carboxylate (1 mmol l^{-1} , dissolved in DMSO) to the internal medium; 6, addition of acetazolamide (0.2 mmol l^{-1}) to the internal bathing medium. The vertical current deflections are due to short voltage pulses and reflect the preparation conductance (G_{te} ; see lower right corner for scale).

during ouabain perfusion reveal interesting differences (see Fig. 2). In gills exhibiting a negative V_{te} , the voltage was reduced to values near 0 mV (Fig. 2A) or the polarity reversed and the gill produced a positive V_{te} (Fig. 2B). In gills showing a positive V_{te} under control conditions, ouabain perfusion increased V_{te} to more positive values (Fig. 2C).

Split gill lamellae: distal side

Distal split lamellae were mounted in a modified Ussing chamber. When perfused on both sides with NaCl saline, this epithelium spontaneously generated a positive voltage (V_{te}) of $+16 \pm 5\text{ mV}$ ($N=6$). Clamping V_{te} to 0 mV gave a negative short-circuit current (I_{sc}) of $-59 \pm 19\text{ }\mu\text{A cm}^{-2}$. The conductance (G_{te}) was $3.80 \pm 0.48\text{ mS cm}^{-2}$. These basic electrophysiological parameters reveal that such preparations consist of the distal epithelium and respective cuticle.

When Cl^- was substituted by nitrate on both sides of the preparation, I_{sc} decreased significantly from -58 ± 18 to $-8 \pm 3\text{ }\mu\text{A cm}^{-2}$ ($N=5$) (Fig. 3). Simultaneously, G_{te} was reduced from 4.05 ± 0.36 to $1.65 \pm 0.34\text{ mS cm}^{-2}$. When Cl^- was restored, a rapid current overshoot resulted, I_{sc} then stabilising at approximately 70% of the original value. In two experiments, Cl^- was initially substituted by nitrate only in the external bath. This almost abolished the negative I_{sc} and markedly reduced G_{te} . Subsequent replacement of Cl^- in the internal bathing medium had no further effect on I_{sc} or G_{te} .

Substitution of Na^+ by choline on both sides of the preparation had a biphasic effect on I_{sc} (Fig. 3). Initially, the negative I_{sc} increased rapidly from a control value of

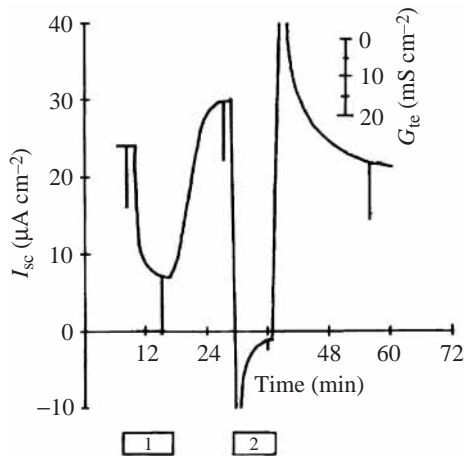


Fig. 4. Representative time course of the short-circuit current (I_{sc}) across a proximal split lamella of a posterior gill with NaCl saline on both sides. The following manipulations are shown: 1, addition of ouabain (2 mmol l^{-1}) to the internal bathing medium; 2, substitution of Na^+ on both sides of the preparation. Substitution and readministration of Na^+ resulted in fast, transient current overshoots (to approximately -40 and $60 \mu\text{A cm}^{-2}$, respectively). These I_{sc} transients are due to concentration gradients resulting from the non-simultaneous replacement of the external and internal bathing media. The vertical current deflections are due to short voltage pulses and reflect the preparation conductance (G_{te} ; see upper right corner for scale).

$-40 \pm 14 \mu\text{A cm}^{-2}$ ($N=5$), reaching a transient maximum at $-82 \pm 12 \mu\text{A cm}^{-2}$. The current then decreased, stabilising at $-49 \pm 15 \mu\text{A cm}^{-2}$. Restoration of Na^+ resulted in a further reduction of the negative I_{sc} to $34 \pm 13 \mu\text{A cm}^{-2}$. The conductances were not significantly affected by Na^+ substitution.

In five experiments, diphenylamine-2-carboxylate (DPC), a Cl^- channel blocker (Di Stefano et al., 1985), was added to the medium representing the haemolymph side (Fig. 3). At 1 mmol l^{-1} , DPC reduced I_{sc} from -28 ± 7 to $-2 \pm 2 \mu\text{A cm}^{-2}$. During DPC washout, I_{sc} recovered to over 80% of the control value. G_{te} was not significantly affected by perfusion of DPC over the internal surface. Dimethylsulphoxide alone, the primary solvent for DPC, had no effect on I_{sc} or G_{te} (Fig. 3). In five experiments, ouabain (2 mmol l^{-1}), a specific inhibitor of the Na^+/K^+ -ATPase (Skou, 1965), was added to the perfusate bathing the haemolymph side of the epithelium for 10–20 min (Fig. 3). Ouabain had no effect on the negative I_{sc} or on G_{te} .

Acetazolamide (0.2 mmol l^{-1}), a carbonic anhydrase inhibitor (Maren, 1967), was added to the internal bathing medium (Fig. 3). Acetazolamide caused a rapid decrease in I_{sc} from -23 ± 7 to $-2 \pm 2 \mu\text{A cm}^{-2}$ ($N=5$). G_{te} was unaffected. The reduction in I_{sc} was only slightly reversible, and the current recovered very slowly during washout.

Split gill lamellae: proximal side

Proximal split lamellae were perfused on both sides with NaCl saline in a modified Ussing chamber. This epithelium

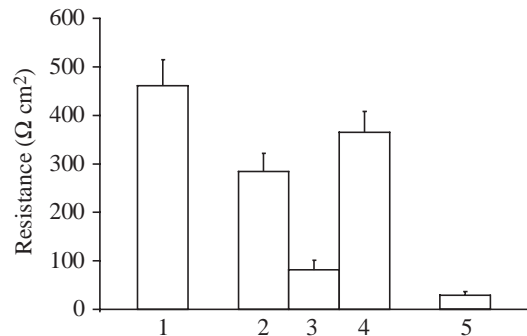


Fig. 5. Diagram showing the electrical resistances ($\Omega \text{ cm}^2$) of different posterior gill preparations: 1, whole gill lamellae ($461 \pm 54 \Omega \text{ cm}^2$, $N=6$); 2, distal split gill lamellae ($284 \pm 38 \Omega \text{ cm}^2$, $N=6$); 3, proximal split gill lamellae ($81 \pm 20 \Omega \text{ cm}^2$, $N=7$); 4, sum of distal and proximal split gill lamellae ($365 \pm 43 \Omega \text{ cm}^2$); 5, isolated cuticles ($29 \pm 7 \Omega \text{ cm}^2$, $N=5$). Values are means \pm S.E.M.

spontaneously generated a negative voltage (V_{te}) of $-5 \pm 2 \text{ mV}$ ($N=7$). Clamping V_{te} to 0 mV gave a positive short-circuit current (I_{sc}) of $+41 \pm 12 \mu\text{A cm}^{-2}$. The conductance (G_{te}) was $18 \pm 5 \text{ mS cm}^{-2}$. These values reveal that the proximal split lamellae consist of the proximal epithelium and cuticle.

Substitution of Na^+ by choline on both sides of the preparations abolished the positive I_{sc} of $+26 \pm 5$ ($-2 \pm 1 \mu\text{A cm}^{-2}$, $N=5$) (Fig. 4). G_{te} was reduced simultaneously from 18 ± 5 to $2.9 \pm 1.0 \text{ mS cm}^{-2}$. The effect of Na^+ substitution was completely reversible.

Addition of ouabain (2 mmol l^{-1}) to the internal bathing medium (Fig. 4) caused a rapid decrease in the positive I_{sc} by approximately 65% from $+24 \pm 5$ to $+8 \pm 4 \mu\text{A cm}^{-2}$ ($N=5$). G_{te} was unaffected by ouabain. The reduction in I_{sc} elicited by ouabain was completely reversible in all experiments.

Whole gill lamellae and cuticle

To evaluate the quality of the split lamella preparations, the electrical resistances of whole gill lamellae and isolated cuticles were measured. Fig. 5 shows these respective resistances together with those of the distal and proximal split lamella preparations and their sum.

Discussion

Haemolymph osmolality and ion concentrations

The haemolymph osmolality of approximately $390 \text{ mosmol kg}^{-1}$ found in the red freshwater crab is low compared with that of other freshwater crabs and lies more within the range of the freshwater *Macrura* (see Table 1). Among the freshwater Crustacea, only the Entomostraca and a few palaemonids have significantly lower haemolymph osmolalities (e.g. *Triops longicaudatus* and *Macrobrachium olfersii*) (Table 1). Given that Na^+ and Cl^- are the major ionic constituents of the haemolymph, it is not surprising that *Dilocarcinus pagei* exhibits low haemolymph concentrations of these ions. Concentrations of K^+ , Ca^{2+} and Mg^{2+} are similar

to those of other freshwater Malacostraca. A reduced haemolymph osmolality could clearly be adaptive, lowering energy expenditure for salt uptake, reducing outwardly directed ionic gradients and, consequently, passive salt loss. In terms of osmotic and ionic gradients, among the freshwater crabs investigated thus far, *Dilocarcinus pagei* appears well suited to life in fresh water.

Microanatomy of the posterior gills

While most Brachyura possess nine pairs of phyllobranchiate gills, the red freshwater crab has only eight (see Fig. 1A,B), although the African freshwater crab *Potamon niloticus* has seven pairs (Maina, 1990). Regions similar to the well-defined, central, dark area in the posterior gill lamellae of *Dilocarcinus pagei* (see Fig. 1D) have been found after silver nitrate staining of the posterior gills of other hyperosmoregulating crabs such as *Callinectes sapidus* (Copeland and Fitzjarrell, 1968), *Carcinus maenas* (Compère et al., 1989) and *Eriocheir sinensis* (Barra et al., 1983). Such areas correspond to a thick epithelium of approximately 10 µm in height showing features typical of transporting cells, including extensive apical and basal membrane infoldings and an elevated mitochondrial density. In *Carcinus maenas* gills, this area increases when the crabs are adapted to a dilute medium (Compère et al., 1989).

A strikingly thick epithelium is also present in the dense region of the posterior gills of *Dilocarcinus pagei*. However, while the lamellar epithelium in marine and brackish water crabs is symmetrically thickened on both lamellar surfaces, and punctuated by occasional pillar cells (Taylor and Taylor, 1992), only the proximal lamellar epithelium is thickened in *Dilocarcinus pagei*. The distal lamellar surface consists of a thin epithelium composed mainly of apical pillar cell flanges. The posterior gill lamellae of *Dilocarcinus pagei* thus exhibit a remarkable epithelial asymmetry (see Fig. 1E,F). The only other histological study on freshwater crab gills revealed that the lamellar epithelia in *Potamon niloticus* gills are symmetrical and that the central, dense region is apparently lacking. The squamous, 6 µm thick, epithelial cells exhibit an extensive system of apical leaflets and basal membrane invaginations associated with mitochondria, which is typical of a structure with transport function (Maina, 1990).

Asymmetrical epithelia resembling those of *Dilocarcinus pagei* occur in the book gill lamellae of the euryhaline horseshoe crab *Limulus polyphemus* (Henry et al., 1996). The ventral epithelium exhibits a thick (5–10 µm), central dense area that displays features characteristic of a transporting epithelium, such as numerous mitochondria associated with basal membrane invaginations and elevated Na⁺/K⁺-ATPase and carbonic anhydrase activities. However, in *Dilocarcinus pagei* lamellae, both epithelia are much thicker (10–20 µm) than in *Limulus polyphemus* lamellae, in which the pillar cell flanges do not constitute the thin epithelium. The irregular pillar cell arrangement in *Dilocarcinus pagei*, where thin apical flanges (see Fig. 1E,F) constitute the distal epithelium, is very similar to that of the lamellar epithelium of freshwater

palaemonid shrimps, which is involved in both gas exchange and ion absorption (Taylor and Taylor, 1992; Freire and McNamara, 1995; McNamara and Lima, 1995; McNamara and Torres, 2000).

Electrophysiological characteristics of posterior gills

Transbranchial voltage (V_{te}) has been measured in a variety of isolated, perfused, whole crustacean gills (see Péqueux et al., 1988). Interestingly, the posterior gills of *Dilocarcinus pagei* generate V_{te} values of different polarity, which are not due to gill position or seasonal variation. V_{te} values of opposite polarity were found on consecutive days and when using gills from the same insertion position (gills 6–8). A novel mechanism of integration of the two different epithelia in the lamellae of individual gills may provide a plausible explanation for these variable V_{te} polarities in the different gills. This hypothesis requires future investigation. In all cases, however, ouabain altered V_{te} to more positive values, indicating inhibition of active, electrogenic Na⁺ absorption generated by the Na⁺/K⁺-ATPase (Fig. 2). The maximum V_{te} values under control conditions for each polarity (–23 and +16 mV, respectively) suggest at least a moderately tight epithelium, as expected for freshwater animals maintaining large ionic gradients.

Split gill lamellae have been used successfully in an Ussing chamber to characterise active NaCl absorption across the gills of hyperosmoregulating Chinese crabs, *Eriocheir sinensis*, and shore crabs, *Carcinus maenas* (for a review, see Onken and Riestenpatt, 1998). In *Dilocarcinus pagei*, the Cl[–]-dependence of the negative I_{sc} and of the transepithelial conductance (G_{te}) of distal split lamellae (see Fig. 3) indicates that the thin epithelium generates active, electrogenic Cl[–] absorption. Negative I_{sc} and G_{te} were not reduced when ouabain was added to the internal bathing medium (see Fig. 3), demonstrating that Cl[–] absorption across this epithelium does not depend on a functioning Na⁺/K⁺-ATPase. Substitution of Na⁺ by choline even increased the negative I_{sc} . Although difficult to interpret at present, this increase does indicate that active Cl[–] absorption is independent of Na⁺. Internal addition of the Cl[–] channel blocker diphenylamine-2-carboxylate (Di Stefano et al., 1985) almost abolished the negative I_{sc} without affecting G_{te} (see Fig. 3). Thus, active Cl[–] absorption seems to proceed *via* basolateral Cl[–] channels, as observed in many other Cl[–]-absorbing epithelia (see Greger and Kunzelmann, 1990). The lack of effect of diphenylamine-2-carboxylate on G_{te} may simply reflect the presence of other electrogenic pathways in the basolateral membrane, the conductance of which, in many epithelia, is determined mainly by K⁺ channels. The internal addition of acetazolamide, a carbonic anhydrase inhibitor (Maren, 1967), reduced the negative I_{sc} , indicating the involvement of carbonic anhydrase in active Cl[–] absorption. These results show striking similarities with active Cl[–] absorption by *Eriocheir sinensis* split gill lamellae (Onken et al., 1991), in which an apical V-type H⁺-pump is thought to drive electrogenic and Na⁺-independent Cl[–] absorption *via* apical Cl[–]/HCO₃[–] antiports and basolateral Cl[–] channels

(Onken and Putzenlechner, 1996). This same transport mechanism seems likely for the thin epithelium of the posterior gill lamellae in *Dilocarcinus pagei*.

The reduction in the positive I_{sc} across proximal split lamellae after the addition of ouabain to the internal bathing medium or after substitution of Na^+ by choline (see Fig. 4) indicates that the thick epithelium generates active, electrogenic Na^+ absorption. As in *Eriocheir sinensis* split gill lamellae (Zeiske et al., 1992), Na^+ absorption may proceed via apical Na^+ channels. Strictly, however, since an apical transport pathway requires confirmation, Na^+ absorption may also proceed via an electrogenic $2\text{Na}^+/\text{H}^+$ antiporter, which has been found in crustacean gill (Shetlar and Towle, 1989) and other transport epithelia (Kimura et al., 1994). In preliminary experiments, external amiloride caused only a minor decrease in current, even at high concentrations (1 mmol l^{-1}). Apparently, this Na^+ channel blocker does not permeate the cuticle and cannot be used to distinguish between channels and antiporters. Substitution of Na^+ by choline not only abolished the positive I_{sc} , but also markedly reduced the conductance to values below 2 mS cm^{-2} (see Fig. 4), indicating that the preparation exhibits a marked selectivity for Na^+ . Such selectivity may be due to the nature of the transporter in the apical membrane and/or to ion-selective paracellular junctions. The cuticle may also contribute, since ion-selectivity by isolated crustacean cuticles has been observed (Lignon and Péqueux, 1990).

A comparison of the resistances of whole gill lamellae with the sum of those of the distal and proximal split lamellae (Fig. 5) reveals a difference of approximately 20%. In particular, the resistance of the thick, proximal epithelium seems to be low. Such preparations generated negative voltages, but these were not as large as those observed with isolated, perfused gills. These data suggest that the proximal split lamellae may suffer some damage during splitting. However, the basic electrophysiological parameters for the distal split lamellae (see Results) demonstrate that these preparations are mainly unaffected by the mechanical splitting process.

The electrophysiological characteristics of the posterior gills of *Dilocarcinus pagei* show clear similarities with those of *Eriocheir sinensis*, a crab that spends most of its life in fresh water. Unlike *Carcinus maenas* (see Riestenpatt et al., 1996), which migrates between sea water and brackish water, both freshwater-inhabiting species generate active, independent, electrogenic absorption of Na^+ and Cl^- . Both apparently possess a tight gill epithelium, which is able to generate high voltages and to maintain large ionic gradients, as expected for freshwater animals. The principal difference in active, transbranchial NaCl absorption between *Dilocarcinus pagei* and *Eriocheir sinensis* lies in the intralamellar distribution of transport functions. The posterior gills of the red freshwater crab actively absorb Na^+ and Cl^- across opposite sides of the lamellae, while the active absorption of Na^+ and Cl^- across Chinese crab gills is effected on both sides.

Transport mechanisms have been proposed for the amphibian skin, fish gills and Chinese crab gills in which two ATPases (an apical H^+ pump and a basolateral Na^+/K^+ -ATPase) drive Na^+ absorption via apical Na^+ channels and Cl^- absorption via apical $\text{Cl}^-/\text{HCO}_3^-$ antiports (Goss et al., 1992; Larsen, 1988; Onken and Riestenpatt, 1998). Although the intraepithelial organisation of the transporters involved appears to be different in these three examples, the model seems to be characteristic of freshwater animals. Absorption of NaCl across the gills of the red freshwater crab apparently conforms to the same principle, although it is manifest in a structurally different manner. It will be a rewarding task to examine this hypothesis and to reveal details of the transport characteristics of *Dilocarcinus pagei* gills in future studies.

The authors gratefully acknowledge financial support from CAPES, CNPq (Brazil) and DAAD (Germany) and photographic assistance by José Augusto Maulin (FMRP, USP).

References

- Barra, J. A., Pequ  ux, A. and Humbert, W. (1983). A morphological study on gills of a crab acclimated to freshwater. *Tissue Cell* **15**, 583–596.
- Comp  re, P., Wanson, S., Pequ  ux, A., Gilles, R. and Goffinet, G. (1989). Ultrastructural changes in the gill epithelium of the green crab *Carcinus maenas* in relation to the external salinity. *Tissue Cell* **21**, 299–318.
- Copeland, D. E. and Fitzjarrell, A. T. (1968). The salt absorbing cells in gills of blue crab (*Callinectes sapidus* Rathbun) with notes on modified mitochondria. *Z. Zellforsch.* **92**, 1–22.
- Di Stefano, A., Wittner, M., Schlatter, E., Lang, H. J., Englert, H. and Greger, R. (1985). Diphenylamine-2-carboxylate, a blocker of the Cl^- conductive pathway in Cl^- -transporting epithelia. *Pfl  gers Arch.* **405**, 95–100.
- Freire, C. A. and McNamara, J. C. (1995). The fine structure of the gills of the freshwater shrimp *Macrobrachium olfersii* (Decapoda): effect of acclimation to high salinity medium and evidence for involvement of the lamellar septum in ion uptake. *J. Crust. Biol.* **15**, 103–116.
- Goss, G. G., Perry, S. F., Wood, C. M. and Laurent, P. (1992). Mechanisms of ion and acid–base regulation in the gills of freshwater fish. *J. Exp. Zool.* **263**, 143–159.
- Greenaway, P. (1981). Sodium regulation in the freshwater/land crab *Holthuisana transversa*. *J. Comp. Physiol. B* **142**, 451–456.
- Greger, R. and Kunzelmann, K. (1990). Chloride-transporting epithelia. In *Basic Principles in Transport, Comparative Physiology*, vol. 3 (ed. R. K. H. Kinne), pp. 84–114. Basel: Karger.
- Harris, R. R. (1975). Urine production rate and urinary sodium loss in the freshwater crab *Potamon edulis*. *J. Comp. Physiol.* **96**, 143–153.
- Henry, R. P., Jackson, S. A. and Mangum, C. P. (1996). Ultrastructure and transport-related enzymes of the gills and coxal gland of the horse shoe crab *Limulus polyphemus*. *Biol. Bull.* **191**, 241–250.
- Kimura, C., Ahearn, G. A., Busquets-Turner, L., Haley, S. R., Nagao, C. and De Couet, H. G. (1994). Immunolocalization of an antigen associated with the invertebrate electrogenic $2\text{Na}^+/\text{H}^+$ antiporter. *J. Exp. Biol.* **189**, 85–104.
- Larsen, E. H. (1988). NaCl transport in amphibian skin. In *Advances in Comparative and Environmental Physiology*, vol. 1 (ed. R. Greger), pp. 189–248. Berlin: Springer.
- Lignon, J. M. and P  queux, A. (1990). Permeability properties of the cuticle and gill ion exchanges in decapod crustaceans. In *Animal Nutrition and Transport Processes. 2. Transport, Respiration and Excretion: Comparative Environmental Aspects. Comparative Physiology*, vol. 6 (ed. J.-P. Truchot and B. Lahlou), pp. 14–27. Basel: Karger.
- Lima, A. G., McNamara, J. C. and Terra, W. R. (1997). Regulation of hemolymph osmolytes and gill Na^+/K^+ -ATPase activities during acclimation to saline media in the freshwater shrimp *Macrobrachium olfersii* (Wiegmann, 1836) (Decapoda, Palaemonidae). *J. Exp. Mar. Biol. Ecol.* **215**, 81–91.

- Magalhães, C. U.** (1991). Revisão taxonômica dos caranguejos dulcícolas da família Trichodactylidae (Crustacea: Decapoda: Brachyura). PhD thesis, Instituto de Biociências, Universidade de São Paulo, Brasil.
- Maina, J. N.** (1990). The morphology of the gills of the freshwater African crab *Potamon niloticus* (Crustacea: Brachyura: Potamonidae): a scanning and transmission electron microscopic study. *J. Zool., Lond.* **221**, 499–515.
- Mantel, L. H. and Farmer, L. L.** (1983). Osmotic and ionic regulation. In *The Biology of Crustacea*, vol. 5 (ed. D. E. Bliss and L. H. Mantel), pp. 54–126. London: Academic Press.
- Maren, T.** (1967). Carbonic anhydrase: chemistry, physiology and inhibition. *Physiol. Rev.* **47**, 595–781.
- McNamara, J. C. and Lima, A. G.** (1995). The route of ion and water movements across the gill epithelium of the freshwater shrimp *Macrobrachium olfersii* (Decapoda, Palaemonidae): evidence from ultrastructural changes induced by acclimation to saline media. *Biol. Bull.* **192**, 321–331.
- McNamara, J. C., Salomão, L. C. and Ribeiro, E. A.** (1990). The effect of eye-stalk ablation on haemolymph osmotic and ionic concentrations during acute salinity exposure in the fresh-water shrimp *Macrobrachium olfersii* (Wiegmann) (Crustacea, Decapoda). *Hydrobiologia* **199**, 193–199.
- McNamara, J. C. and Torres, A. H.** (1999). Ultracytochemical localization of Na⁺/K⁺-ATPase activity and effect of high salinity acclimation in gill and renal epithelia of the freshwater shrimp *Macrobrachium olfersii* (Crustacea, Decapoda). *J. Exp. Zool.* **284**, 617–628.
- Morris, S. and Van Aardt, W. J.** (1998). Salt and water relations, and nitrogen excretion, in the amphibious freshwater crab *Potamonautes warreni* in water and in air. *J. Exp. Biol.* **201**, 883–893.
- Onken, H., Graszynski, K. and Zeiske, W.** (1991). Na⁺-independent electrogenic Cl⁻ uptake across the posterior gills of the Chinese crab (*Eriocheir sinensis*): Voltage-clamp and microelectrode studies. *J. Comp. Physiol. B* **161**, 293–301.
- Onken, H. and Putzenlechner, M.** (1996). A V-ATPase drives active, electrogenic and Na⁺-independent Cl⁻ absorption across the gills of *Eriocheir sinensis*. *J. Exp. Biol.* **198**, 767–774.
- Onken, H. and Riestenpatt, S.** (1998). NaCl absorption across split gill lamellae of hyperregulating crabs: Transport mechanisms and their regulation. *Comp. Biochem. Physiol.* **119A**, 883–893.
- Péqueux, A.** (1995). Osmotic regulation in crustaceans. *J. Crust. Biol.* **15**, 1–60.
- Péqueux, A., Gilles, R. and Marshall, W. S.** (1988). NaCl transport in gills and related structures. In *Advances in Comparative and Environmental Physiology*, vol. 1 (ed. R. Greger), pp. 1–73. Berlin, Heidelberg: Springer.
- Potts, W. T. W. and Parry, G.** (1964). *Osmotic and Ionic Regulation in Animals*. Oxford: Pergamon Press. 423pp.
- Riestenpatt, S., Onken, H. and Siebers, D.** (1996). Active absorption of Na⁺ and Cl⁻ across the gill epithelium of the shore crab *Carcinus maenas*: voltage-clamp and ion-flux studies. *J. Exp. Biol.* **199**, 1545–1554.
- Santos, F. H. and McNamara, J. C.** (1996). Neuroendocrine modulation of osmoregulatory parameters in the freshwater shrimp *Macrobrachium olfersii* (Wiegmann) (Crustacea, Decapoda). *J. Exp. Mar. Biol. Ecol.* **206**, 109–120.
- Schwarz, H.-J. and Graszynski, K.** (1989). Ion transport in crab gills: A new method using isolated half platelets of *Eriocheir* gills in an Ussing-type chamber. *Comp. Biochem. Physiol.* **92A**, 601–604.
- Shaw, J.** (1959). Salt and water balance in the East African freshwater crab, *Potamon niloticus* (M. Edw.). *J. Exp. Biol.* **36**, 157–179.
- Shetlar, R. E. and Towle, D. W.** (1989). Electrogenic sodium-proton exchange in membrane vesicles from crab (*Carcinus maenas*) gill. *Am. J. Physiol.* **257**, R924–R931.
- Skou, J. C.** (1965). Enzymatic basis for active transport of Na⁺ and K⁺ across cell membrane. *Physiol. Rev.* **45**, 596–617.
- Taylor, H. H. and Taylor, E. W.** (1992). Gills and lungs: the exchange of gases and ions. In *Microscopic Anatomy of Invertebrates*, vol. 10, *Decapod Crustacea* (ed. W. F. Harrison and A. G. Humes), pp. 203–293. New York: Wiley-Liss, Inc.
- Zeiske, W., Onken, H., Schwarz, H.-J. and Graszynski, K.** (1992). Invertebrate epithelial Na⁺ channels: Amiloride-induced current-noise in crab gill. *Biochim. Biophys. Acta* **1105**, 245–252.